

We are IntechOpen, the world's leading publisher of Open Access books Built by scientists, for scientists

6,900

Open access books available

185,000

International authors and editors

200M

Downloads

Our authors are among the

154

Countries delivered to

TOP 1%

most cited scientists

12.2%

Contributors from top 500 universities



WEB OF SCIENCE™

Selection of our books indexed in the Book Citation Index
in Web of Science™ Core Collection (BKCI)

Interested in publishing with us?
Contact book.department@intechopen.com

Numbers displayed above are based on latest data collected.
For more information visit www.intechopen.com



Interaction of Sandy Islands

Takaaki Uda, Masumi Serizawa and Shiho Miyahara

Abstract

The formation of land-tied islands as a result of the extension of a cusped foreland, when waves were incident to several islands composed of sand from two opposite directions, was first investigated, taking a land-tied island offshore of Shodoshima Island in the Seto Inland Sea, Japan, as an example, and their topographic changes were predicted using the Type 5 BG model. Then, the interaction among multiple circular sandy islands on flat shallow seabed owing to waves was investigated, taking the islands in Hingham Bay near Boston Harbor as an example. On the basis of this example, topographic changes were also predicted using the Type 5 BG model.

Keywords: land-tied island, interaction of islands, Shodoshima Island, multiple islands, Hingham Bay

1. Introduction

When waves are incident to a sandy beach from two opposite directions, a cusped foreland may develop, and a land-tied island could be formed by the extension of a cusped foreland. A typical land-tied island can be seen offshore of Shodoshima Island in the Seto Inland Sea, Japan [1]. This land-tied island extends from Bentenjima to Oyoshima Islands with two small islands, Nakayoshima and Koyoshima Islands, between them (**Figures 1** and **2**). The island and mainland are combined by a slender sandbar, which is exposed during low tide, suggesting that wave action from both sides of the sandbar balances each other. The sandbars connecting these islands are popular tourist attractions because of the scenic beauty, and understanding the formative mechanism is important in the study of the preservation of the sandbar. The formation of a land-tied island, however, has not been studied in the previous works except the studies regarding the morphological features of the fully developed land-tied island. In this chapter, field observations were first carried out around Oyoshima Island, and then the elongation of a sandbar of a land-tied island was predicted using the Type 5 BG model while focusing the importance of the wave-sheltering effect of an island affecting to another island into account. Then, the interaction among multiple circular sandy islands on flat shallow seabed owing to waves was investigated, taking the islands in Hingham Bay near Boston Harbor as an example. On the basis of this example, topographic changes were predicted using the Type 5 BG model.



Figure 1.
Location of study area on the south shore of Shodoshima Island.

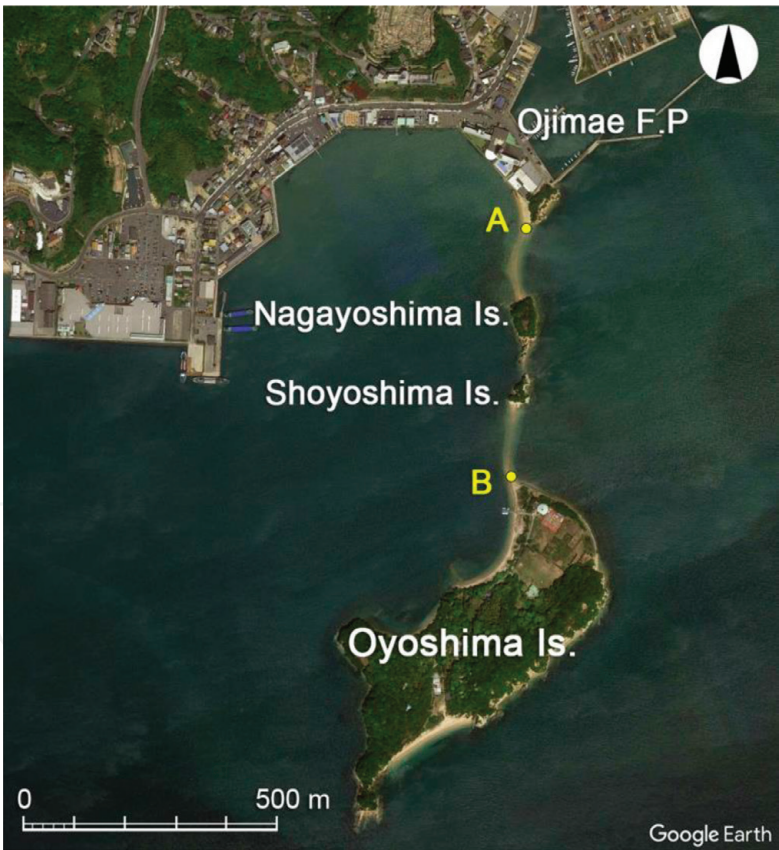


Figure 2.
A sandbar of land-tied island extending between Shodoshima and Oyoshima Islands.

2. Prediction of formation of land-tied islands

2.1 Field observations on Oyoshima Island

Field observation on this land-tied island was carried out during low and high tides on April 26 and 27, respectively, in 2013 [1]. In this area, two small isolated

islands, Nakayoshima and Shoyoshima Islands, are also located between the islands (Figure 2). The primary study area is the sandbar extending between the Ojima fishing port and Oyoshima Island.

Figures 3 and 4 show views of the sandbar extending from the mainland to Nakayoshima Island, taken from the top of Bentenjima Island (A in Figure 2) during low and high tides, facing the south. On the west side of the sandbar, a seabed of a gentle slope covered with gravel extended. Although the top of the sandbar was exposed during low tide, it was immediately below the sea surface during high tide. In addition, the sandbar had developed along the eastern marginal line of a shallow gravel bed of a gentle slope. In contrast, the beach on the east side of the sandbar

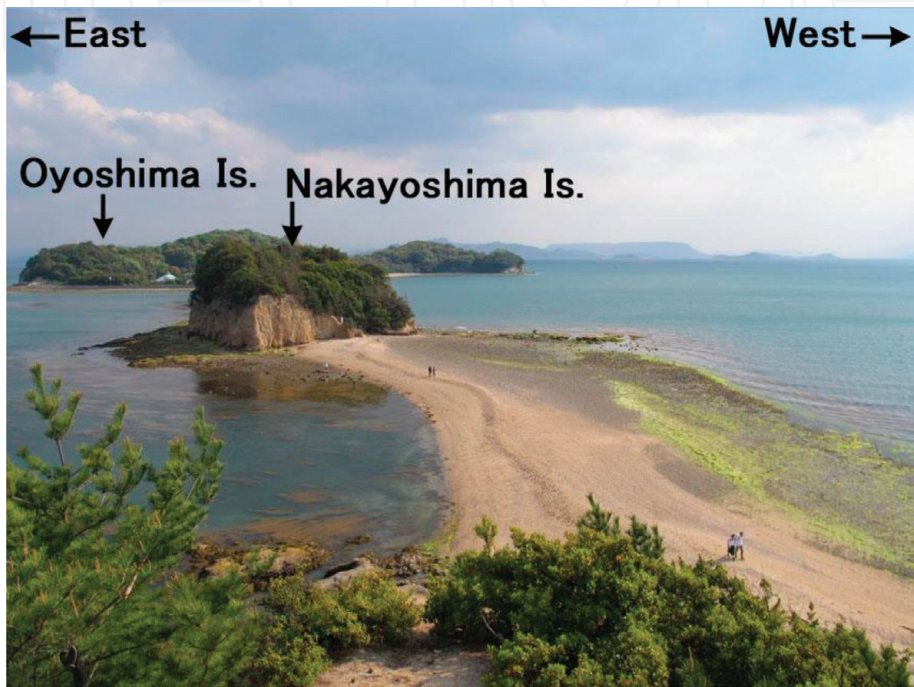


Figure 3.
Oblique photograph of sandbar taken during low tide on April 26, 2013 [1].

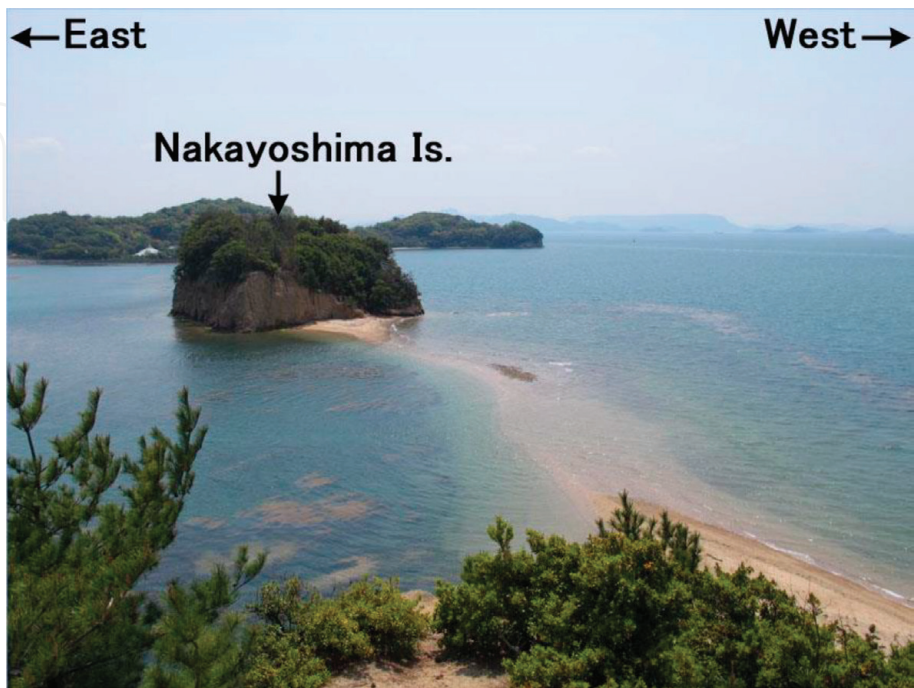


Figure 4.
Oblique photograph of sandbar taken during high tide on April 27, 2013 [1].



Figure 5.
Foreshore slope of 1/6.3 measured at the north side of Nakayoshima Island [1].

had a steep slope with concave shoreline, and exposed rocks covered with seaweed were observed offshore of the sandbar, implying no sand movement.

On Nakayoshima Island, a sea cliff and a wide wave-cut bench can be seen on the east side, in contrast to a lack of abrasion on the west side of the island, implying that the wave intensity from the east is greater than that from the west because of the longer fetch distance to the east (**Figure 2**). The beach material was composed of well-sorted granite sand supplied from sea cliffs composed of unconsolidated granite layers.

The foreshore of the sandbar elongating from the west end of Bentenjima to Nakayoshima Islands was composed of granite coarse sand, and the foreshore slope was 1/6.3 (**Figure 5**). On the east side of Nakayoshima Island, sea cliff and wave-cut bench were formed (**Figure 6**). The sea cliff is the highest at the east end with a gradually decreasing height westward and was composed of a well-weathered granite layer. It was inferred from these observations that Nakayoshima Island itself was a sand source for littoral sediment necessary for forming the land-tied island, and sand is mainly supplied from the east side of the island.

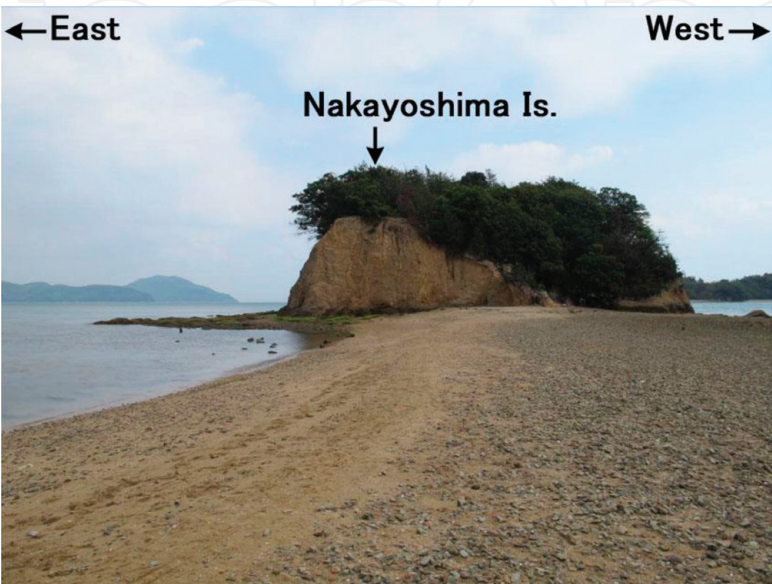


Figure 6.
Sea cliff and wave-cut bench on the east side of Nakayoshima Island [1].

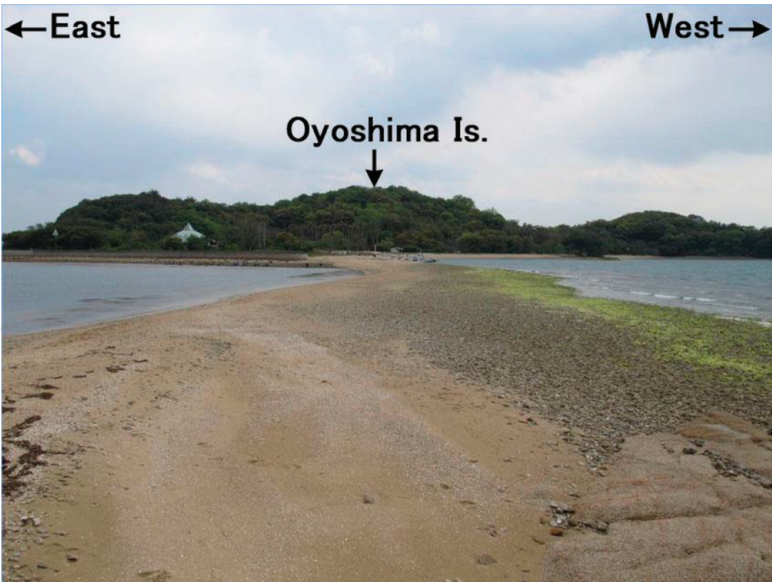


Figure 7.
Sandbar extending between Shoyoshima and Oyoshima Islands [1].

At the south end of Shoyoshima Island, a sandbar extended toward Oyoshima Island (**Figure 7**), and the sandbar extended along the eastern edge of the gravel bed. At the north end of Oyoshima Island (point B in **Figure 2**), granite sand was deposited on the gravel bed composed of andesite (**Figure 8**). Furthermore, although the sandbar of a land-tied island of Oyoshima is convex to the west, the formation of this convex shape is assumed to be due to the greater intensity of the waves from the east relative to that from the west because of the longer fetch distance to the east (**Figure 2**).

2.2 Calculation conditions

Four cases of calculations were carried out. Consider a rectangular area with 600 m length in the longshore and cross-shore directions in Cases 1, 2, and 3 and 2000 and 500 m in longshore and cross-shore directions in Case 4. A flat shallow body of water with a constant depth of 3 m was assumed. Irregular waves were assumed to



Figure 8.
Sandbar extending between Oyoshima and Shoyoshima Islands [1].

be incident from the upper and lower sides of the calculation domain, and the topographic changes associated with the formation of a land-tied island were predicted using the Type 5 BG model [1]. Two sand sources were placed on both sides of the calculation domain in Cases 1 and 2, which had different probabilities of the occurrence of waves from two opposite directions, 1:1 and 1:0.5 in Cases 1 and 2, respectively. In Case 3, two sand sources were alternately placed on both sides of the calculation domain with the same probability of the occurrence of waves from two opposite directions as in Case 1. In Case 4, a sand source modeling a sea cliff on Nakayoshima Island was set at the center of the calculation domain with three small islands on each side of the sand source. To model the sand supply from the sea cliffs, the sand deficit was supplied at each step to maintain the topography of the sand source over time.

The wave direction at each step was randomly determined given the probability of the occurrence of the wave direction, similarly to the method given by San-nami et al. [2]. As the probability distribution of the occurrence of waves incident from two opposite directions, the energy distribution for multidirectional irregular waves with a directional spreading parameter of $S_{max} = 10$ was used. **Table 1** summarizes the conditions for calculating land-tied islands. In the calculation, waves were incident with a probability from all the directions on both sides of a land-tied island. The wave-sheltering effect increases around an island or the sandbar, and this enhances the sand deposition in the wave-shelter zone, and, in turn, sand deposition further increases the wave-sheltering effect (positive feedback).

2.3 Calculation results

When sand sources were set on both sides of the calculation domain and irregular waves with a significant wave height of 1 m were incident from the upper and lower sides of the calculation domain with the same probability of occurrence as in Case 1, a pair of cusplate forelands extended, and then a straight sandbar was formed (**Figure 9**). In Case 2 with the asymmetric probability of occurrence of 1:0.5, two cusplate forelands oriented downward were formed at the initial stage. They approached each other, and after 1.2×10^4 h, a sandbar was formed with a convex upper shoreline (**Figure 10**). Thus, when the probability of occurrence of waves was different, the effect of the asymmetric wave incidence was left in the asymmetric form of a cusplate foreland and a land-tied island. These results are in good agreement with the measured results, where the sandbar connecting

Calculation method		Type 5 BG model
Incident wave height H		1 m
Berm height h_R		1 m
Depth of closure h_c		3 m
Equilibrium slope $\tan \beta_c$		1/10
Coefficients of sand transport	Longshore and cross-shore sand transport coefficient $K_s = 0.2$	
Mesh size		$\Delta x = \Delta y = 10$ m
Time interval		$\Delta t = 2$ h
Duration of calculation		8×10^4 h (4×10^4 steps)
Boundary conditions	Shoreward and landward ends $q_x = 0$ Right and left boundaries $q_y = 0$	

Table 1.
conditions for calculating land-tied islands.

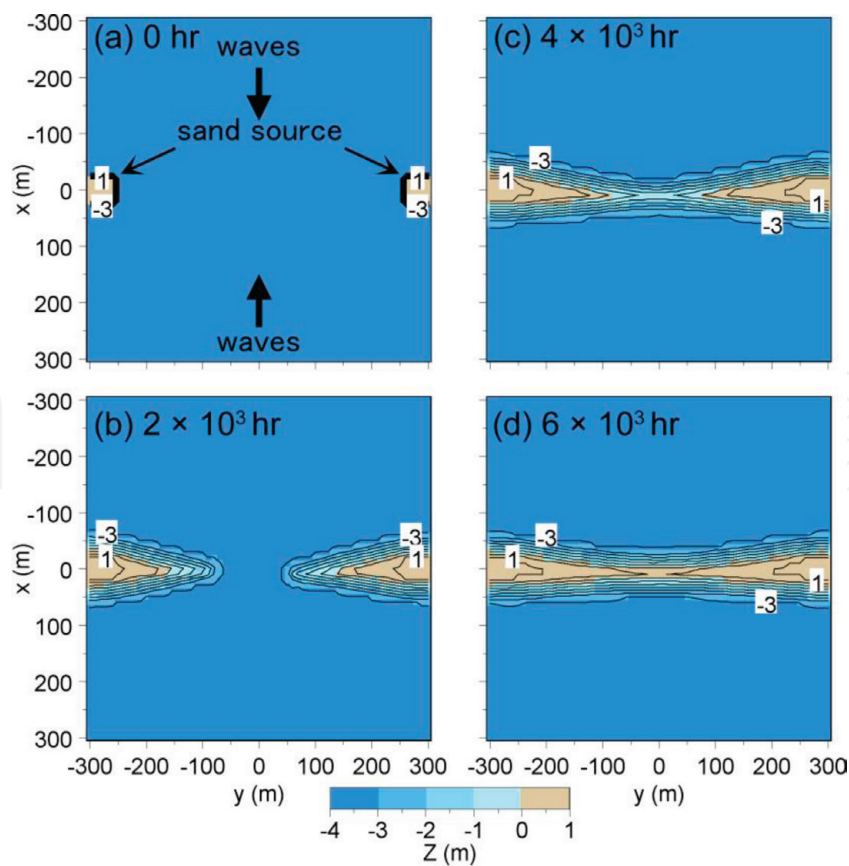


Figure 9.
Calculation results of Case 1 [1].

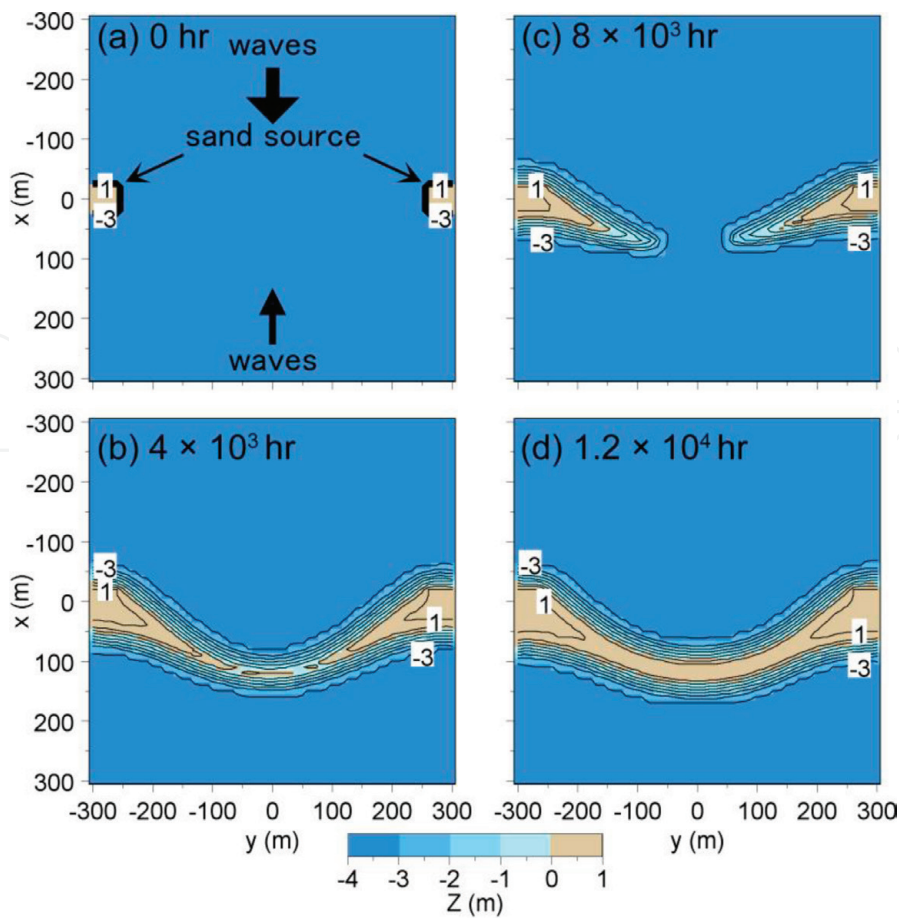


Figure 10.
Calculation results of Case 2 [1].

Bentenjima and Oyoshima Islands had a concave shape on the east side, as shown in **Figure 2**, implying that the wave intensity from the east is greater than that from the west.

When two sand sources were alternately placed on both sides of the calculation domain as in Case 3, the cusped forelands on both sides pulled at each other owing to the wave-sheltering effect and the sandbars connected. Finally, an oblique cusped foreland was formed after 2×10^4 h (**Figure 11**). In Case 4, the elongation of a sandbar was predicted, as shown in **Figure 12**. A slender sandbar extended from the sand source behind the islands owing to the wave-sheltering effect of islands a and a' after 8×10^3 h, and the sand deposition zone extended toward islands b and b' after 1.6×10^4 h. The tip of the sandbar reached the ends of islands b and b' after 2.4×10^4 h, and the sandbar extended beyond islands b and b' up to 3.2×10^4 h. Finally, the sandbar reached islands c and c' located at both ends of the calculation domain after 4×10^4 h. The connection of the small islands by a slender sandbar convincingly explains the elongation of the sandbar connecting Oyoshima Island.

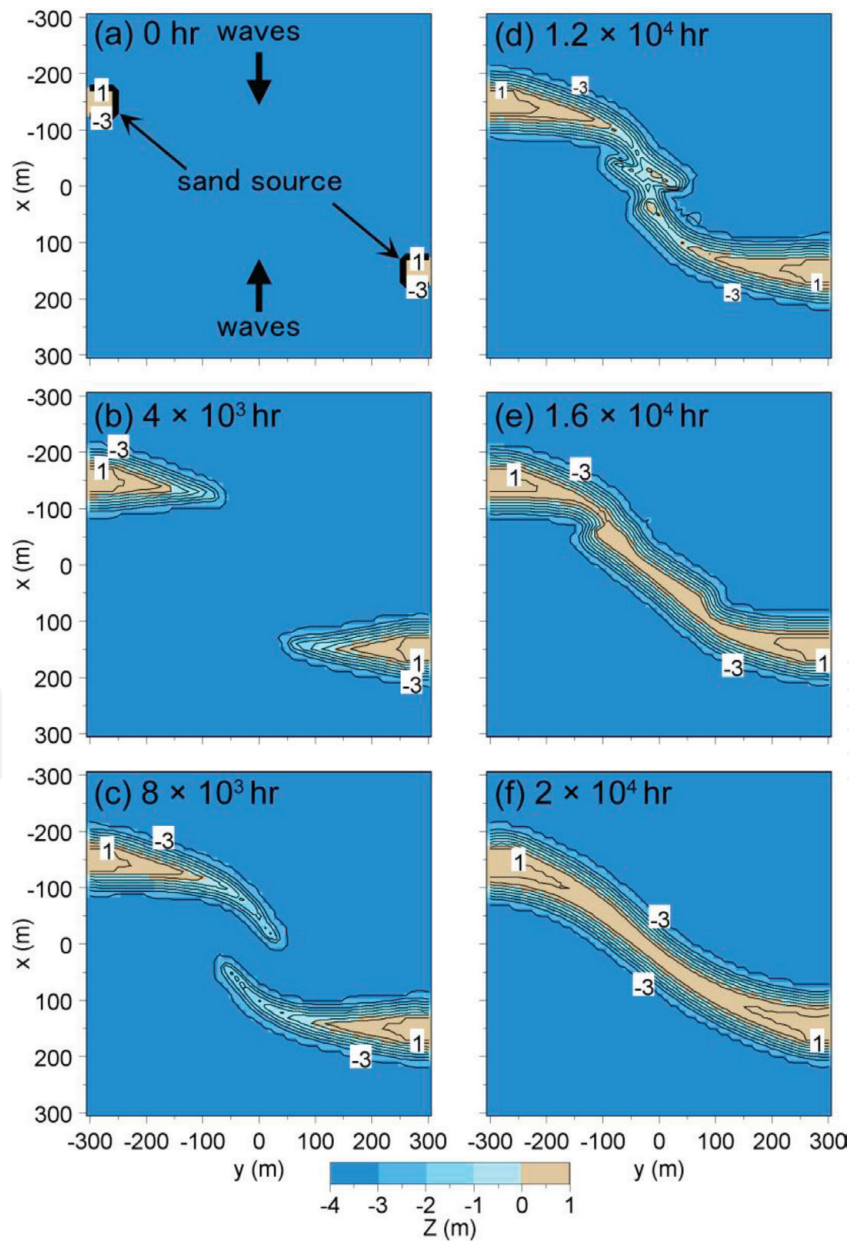


Figure 11.
Calculation results of Case 3 [1].

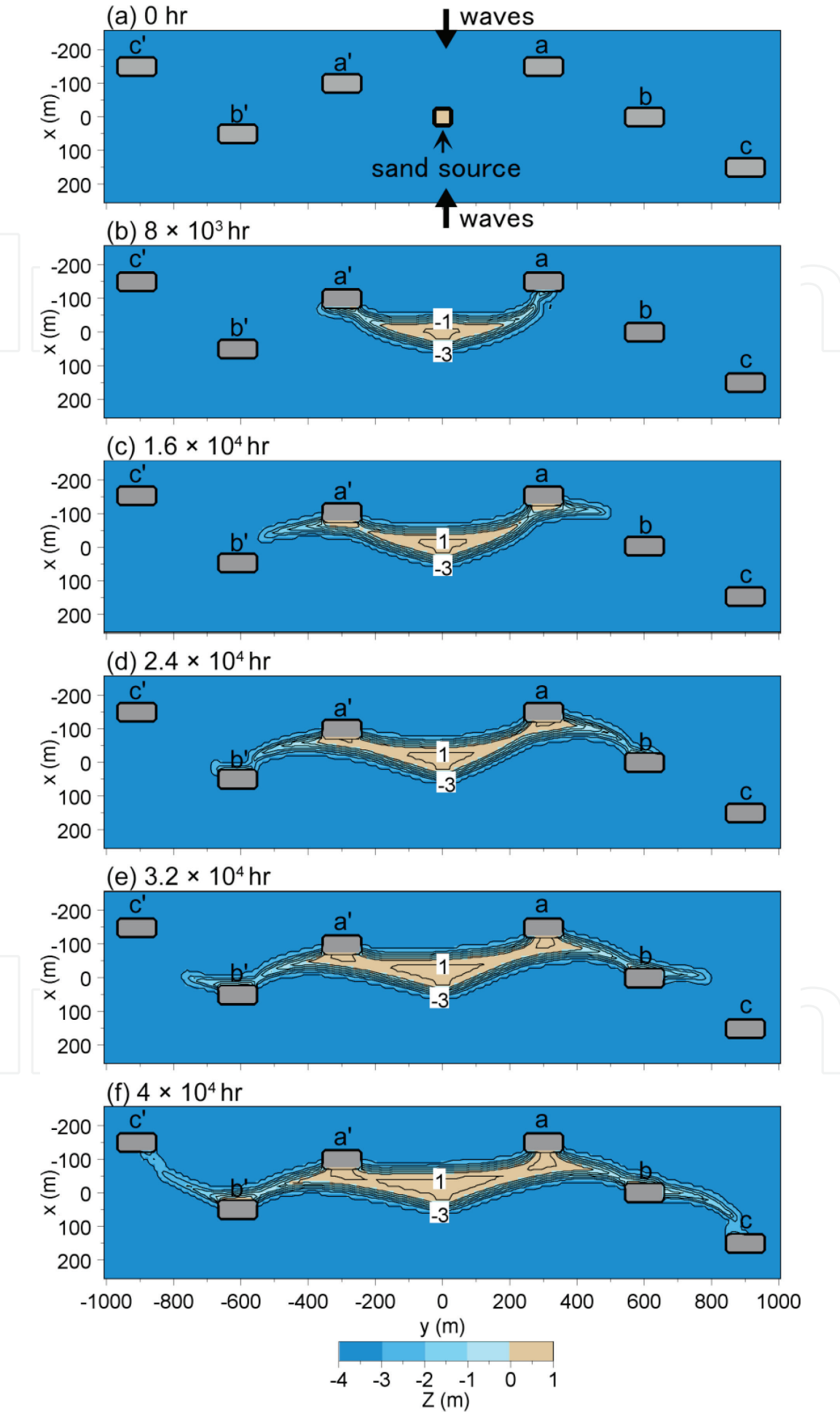


Figure 12.
Calculation results of Case 4 [1].

3. Interaction among multiple circular sandy islands on flat shallow seabed owing to waves

3.1 Connected islands in Hingham Bay in Massachusetts

Figure 13 shows the satellite image of Hingham Bay near Boston Harbor, where Davis and Fitzgerald [3] investigated the formation of Nantasket Beach, and the enlarged images of rectangular areas 1 and 2 in **Figure 13** are shown in **Figures 14** and **15** [3]. In area 1, small island A is seemed to connect to another island B with a slender sandbar, resulting in the formation of Rainsford Island. Similarly, in area 2, four small islands A, B, C, and D connected each other by slender sandbars, resulting in the formation of Peddocks Island. These examples imply that a sandbar may extend in a shallow water body among the islands and small islands may connect with each other by a slender sandbar, suggesting the importance of the wave-sheltering effect of islands themselves.

3.2 Calculation conditions

To investigate the deformation and interaction of multiple islands composed of sand by wave action in a shallow sea, the circular sandy islands were set on a plane solid seabed with a water depth of 2 m, and the beach changes were predicted in Cases 1 and 2 [4]. In both cases, wave incidence from the direction ranging between 0° and 360° with the same probability was assumed. In Case 3, the formation of Peddocks Island in Hingham Bay, as shown in **Figure 15**, was predicted. Since Peddocks Island is assumed to be composed of four islands, four circular islands with the radii of 250 m (A and B), 400 m (C), and 150 m (D) were assumed as the initial condition. The elevation of these islands and water depth surrounding the islands were assumed to be 1 and 2 m, respectively, with the same beach slope of 1/10 and wave conditions as those in Cases 1 and 2. Waves are assumed to be incident to these islands from all the directions with the same probability.

The incident wave height $H_{1/3}$ was assumed to be 1 m. Taking into consideration that the beach changes occur in extremely shallow water, the depth distribution



Figure 13.
Satellite image of Hingham Bay in Massachusetts.



Figure 14.
Satellite image of area 1 (Rainsford Island) in Hingham Bay.



Figure 15.
Satellite image of area 2 (Peddocks Island) in Hingham Bay.

of the sand transport was assumed to be uniform. The conditions for calculating deformation and interaction of multiple islands are summarized in **Table 2**.

3.3 Calculation results

3.3.1 Interaction of sandy islands of symmetric form

In Case 1, the wave-sheltering effect was induced by the sandy islands themselves [4]. Consider two sandy islands with the origin at points of $(x, y) = (0, 200)$

Calculation method	Type 5 BG model
Incident wave height $H_{1/3}$	1 m
Berm height h_R	1 m
Depth of closure h_c	2 m
Equilibrium slope $\tan \beta_c$	1/10
Coefficients of sand transport	Coefficient of longshore and cross-shore sand transport $K_s = 0.2$
Mesh size	$\Delta x = \Delta y = 10 \text{ m}$
Time intervals	$\Delta t = 1 \text{ h}$
Duration of calculation	$3.5 \times 10^4 \text{ h}$ (3.5×10^4 steps)
Boundary conditions	Shoreward and landward ends $q_x = 0$ Right and left boundaries $q_y = 0$

Table 2.
Conditions for calculating deformation and interaction of multiple islands.

and $(0, -200)$ and with the radius of 100 m (**Figure 16**). It is assumed that the two islands have the same size; the elevation and beach slope of the islands are 1 m and 1/10, respectively; and the two islands exist in a shallow sea of 2 m depth. Waves are assumed to be incident to these islands from all the directions with the same probability.

Under these conditions, island A is subject to the wave-sheltering effect by island B when waves are incident from the direction of the positive y -axis as in **Figure 17** [4]. Similarly, island B is subject to the wave-sheltering effect by island A when waves are incident from the direction of the negative y -axis. In contrast, when waves are incident from $\pm x$ -axis direction, the wave field around islands A and B is not subject to the wave-sheltering effect of either island. Because waves are incident from all the directions around the islands, if the wave direction has a $\pm y$ component, island A or B is subject to the wave-sheltering effect by island B or A, respectively. Since the offshore breakwater is located at a fixed position, the offshore breakwater creates a stationary wave-shelter zone behind the structure, whereas in the case of multiple islands, the islands producing the wave-sheltering effects themselves may deform, resulting in a temporal change in the wave-sheltering effect. These are the major differences in both cases [4].

Under the conditions mentioned above, slender sandbars started to extend from the islands in the direction opposite to each other between the islands (**Figure 16**). After 2×10^3 steps, the sandbars extended from islands A and B almost connected with each other (**Figure 16(c)**), and the two islands became a single island with a neck in the center until 5×10^3 steps (**Figure 16(d)**). As time further elapsed, the neck in the center gradually disappeared, and the island was reduced to an elliptic form. After 2×10^4 steps, an island of almost elliptic form was formed with a center at a point of $(x, y) = (0, 0)$ (**Figure 16(f)**).

3.3.2 Interaction of two sandy islands of asymmetric form

In Case 2, the islands of different sizes were considered [4]. Because the wave-sheltering effect of a large island is more effective than that of a small island, asymmetric beach changes may occur. Two circular sandy islands A and B both centered at points of $(x, y) = (0, 200)$ and $(0, -200)$ and with radii of 100 m (A) and 50 m (B) were considered (**Figure 18**). The elevation of the islands and water depth surrounding the islands were assumed to be 1 and 2 m, respectively, with the same beach slope of 1/10 and wave conditions as those in Case 1.

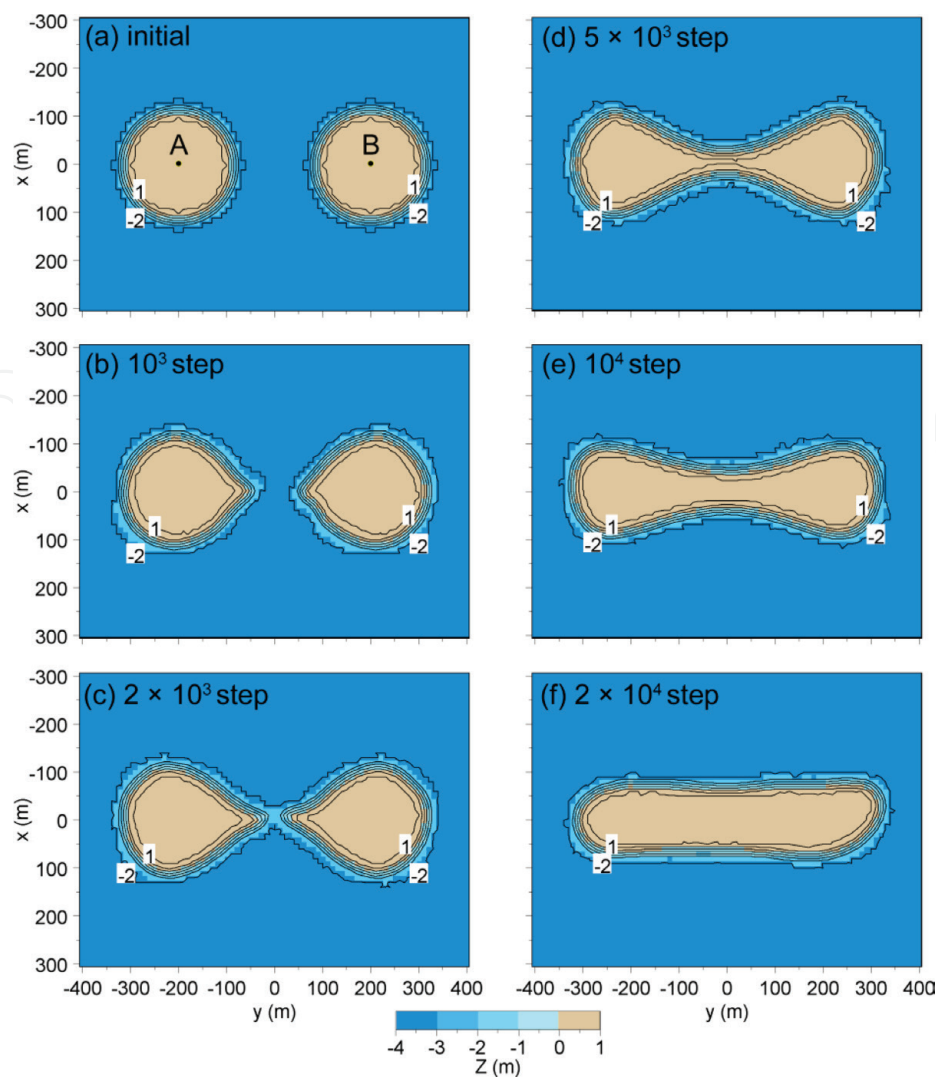


Figure 16.
Deformation and interaction of two symmetric islands composed of sand [4].

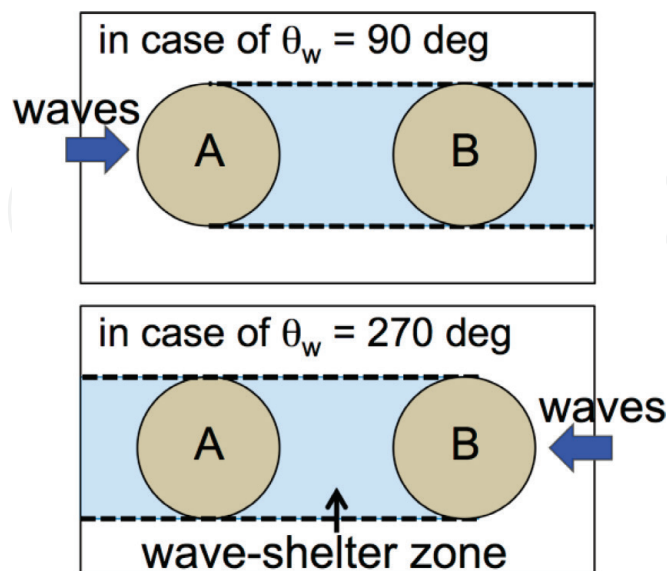


Figure 17.
Schematic view of wave-shelter zone behind two islands of same size under alternate wave incidence [4].

Under these conditions, island A is subject to the wave-sheltering effect of island B when waves are incident from the direction of the positive y -axis, but the wave-sheltering effect is relatively weak because of the smaller size of island B (**Figure 19**) [4].

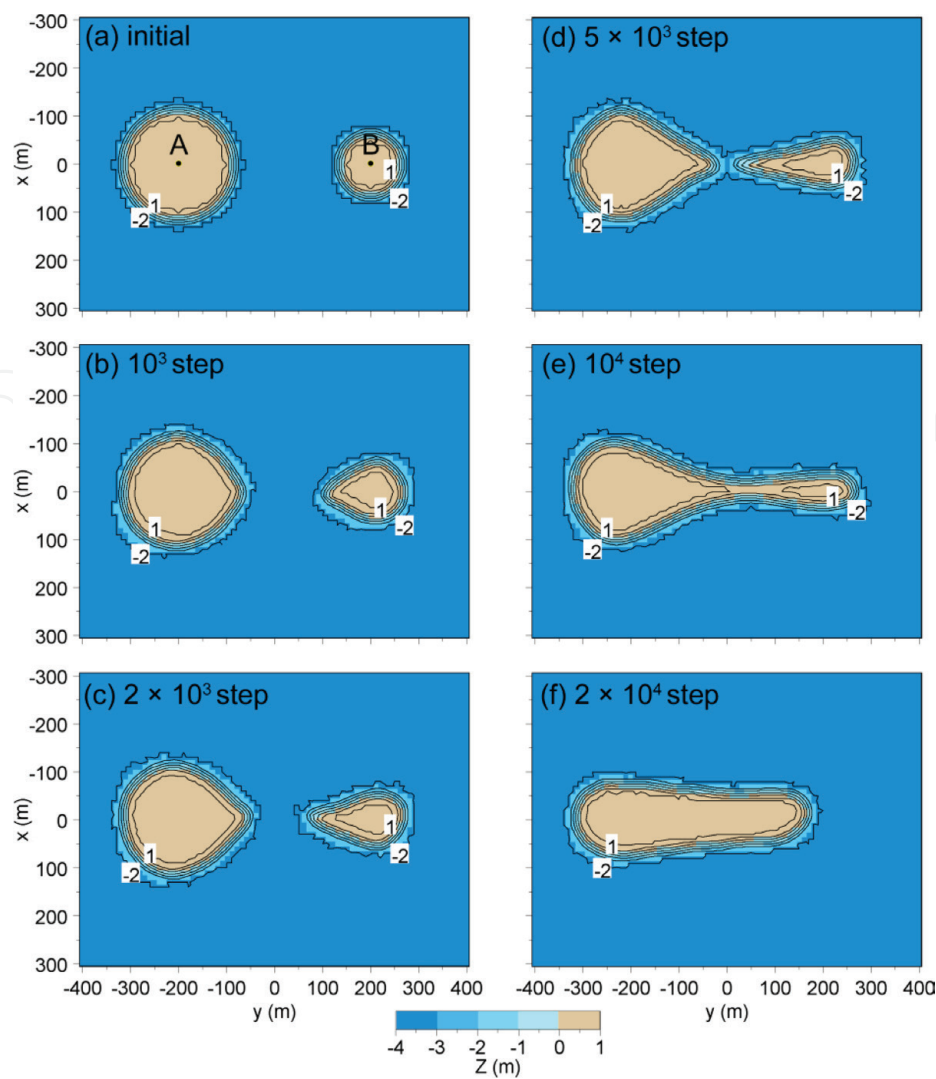


Figure 18.
Deformation and interaction of two asymmetric sandy islands [4].

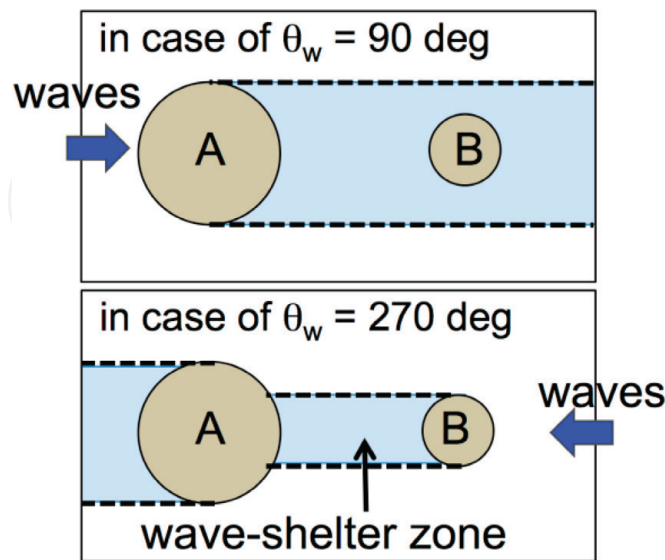


Figure 19.
Schematic view of wave-shelter zone behind small and large islands under alternate wave incidence [4].

On the other hand, when waves are incident from the direction of the negative y -axis, island B is subject to the stronger wave-sheltering effect of island A because of the larger size of island A than island B. Since waves are incident from all the directions around the

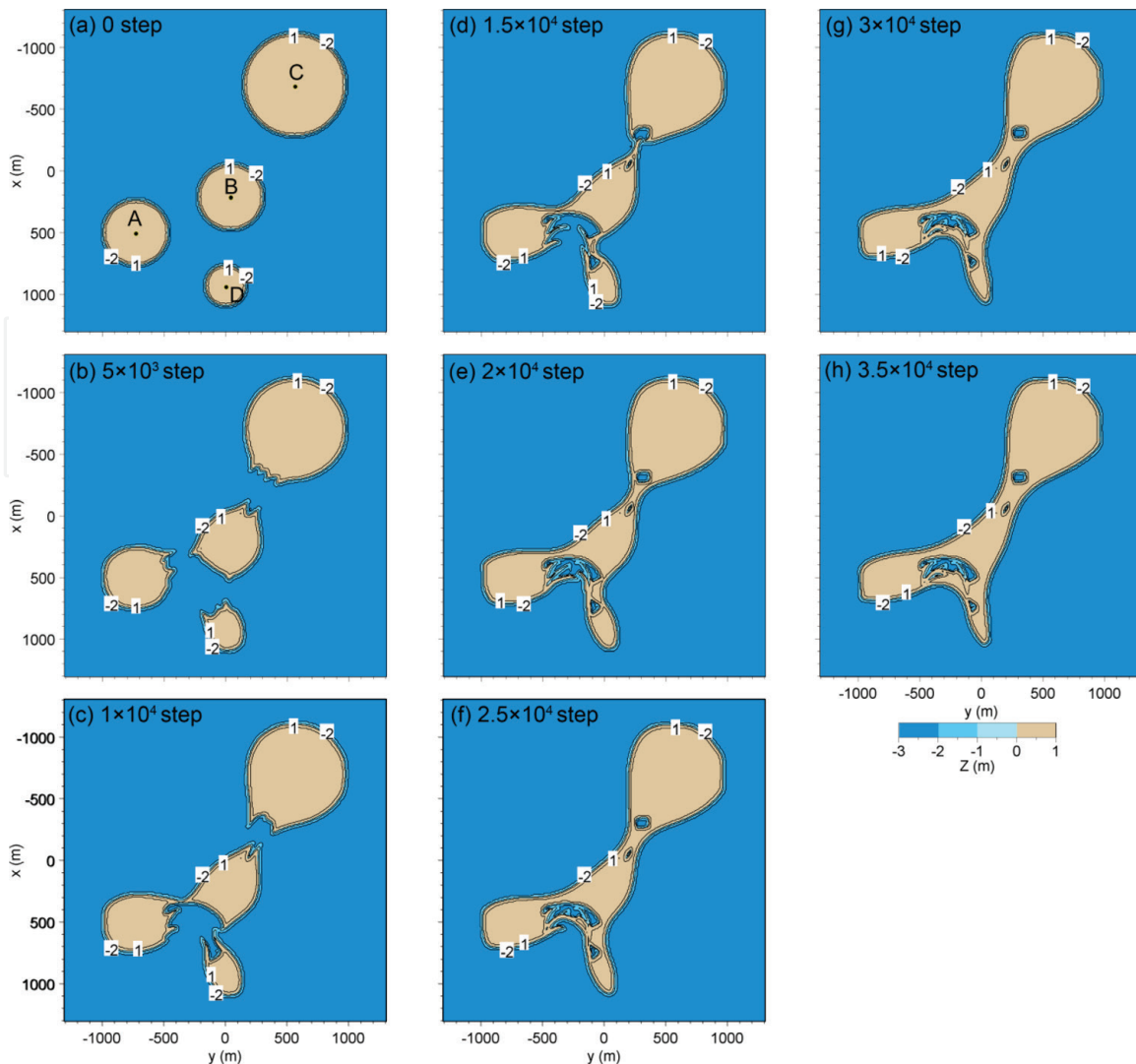


Figure 20.
 Numerical simulation of formation of Peddocks Island in Hingham Bay.

islands, if the wave direction has a $\pm y$ component, island A or B is subject to the wave-sheltering effect by island B or A, respectively, but the wave-sheltering effect always becomes asymmetric.

The cusped foreland started to extend in opposite directions between the islands, resulting in the larger cusped foreland of island B to island A because island B is subject to the stronger wave-sheltering effect of island A (**Figure 18**) [4]. After 5×10^3 steps, the two islands extended and almost connected with each other (**Figure 18(d)**). After 10^4 steps, a slender sandbar, the width of which decreases rightward, was formed (**Figure 18(e)**). After a large number of time steps, the island became elliptical in shape, and the center of the island moved as a whole near the point of $(x, y) = (-100, 0)$ leftward compared with in Case 1 that the size of the islands is equivalent. Thus, the wave-sheltering effect of the islands themselves played an important role in the deformation of the islands located in shallow sea.

3.3.3 Prediction of formation of Peddocks Island in Hingham Bay

Figure 20 shows the results of the calculation. Four circular islands at the initial stage started to pull each other, and slender sandbars started to extend between the islands by 10^4 steps (**Figure 20(c)**). After 1.5×10^4 steps, four islands connected each other owing to the extension of a slender sandbars (**Figure 20(d)**). After 2×10^4 steps, the width of the sandbars increased (**Figure 20(e)**), and up to 3.5×10^4 steps,

four islands connected each other (**Figure 20(h)**), similar to the case of Peddocks Island, as shown in **Figure 15**. Although a small closed water body is left in **Figure 15** between islands A and B, the formation of such a closed water body was successfully predicted, as shown in **Figure 20**.

4. Conclusions

In Chapter 6, three topics were discussed, and topographic changes were predicted using the Type 5 BG model: (1) formation of land-tied islands, (2) interaction among multiple circular sandy islands on flat shallow seabed owing to waves, and (3) prediction of formation of Peddocks Island in Hingham Bay.

1. Field observation was carried out around the land-tied islands of Oyoshima, and the elongation of a sandbar connecting land-tied islands was successfully predicted by the Type 5 BG model when the wave direction at each step was randomly determined given the probability of occurrence of the wave direction [1]. It was concluded that the wave-sheltering effect of the islands and the shallowness of the body of water were key factors for the extension of a slender sandbar and the formation of a land-tied island.
2. The deformation and interaction of multiple sandy islands in a flat shallow sea offshore of Nantasket Beach in Massachusetts [3] were investigated, and the 3-D beach changes and interactions of these multiple islands were successfully predicted.
3. Peddocks Island in Hingham Bay was assumed to be composed of four circular islands at the initial stage with the radii of 250 m (A and B), 400 m (C), and 150 m (D). Then, the present form of Peddocks Island was predicted using the Type 5 BG model. The shape of Peddocks Island as well as the formation of a closed water body between small islands was successfully predicted.

As further application of the Type 5 BG model to the prediction of beach changes, the model was used to predict the elongation and connection of sandbars located offshore of Krabi in Thailand under waves [5].

Acknowledgements

Parts of the contents described in Chapter 6, that is, (1) prediction of formation of land-tied islands and (2) interaction among multiple circular sandy islands on flat shallow seabed owing to waves, are based on the articles [1, 4] presented at the 34th Conference on Coastal Engineering, Seoul, Korea (2014). We would like to express our gratitude for the use of materials.

IntechOpen

Author details


Takaaki Uda^{1*}, Masumi Serizawa² and Shiho Miyahara²

¹ Public Works Research Center, Tokyo, Japan

² Coastal Engineering Laboratory Co., Ltd., Tokyo, Japan

*Address all correspondence to: uda@pwrc.or.jp

IntechOpen

© 2018 The Author(s). Licensee IntechOpen. Distributed under the terms of the Creative Commons Attribution - NonCommercial 4.0 License (<https://creativecommons.org/licenses/by-nc/4.0/>), which permits use, distribution and reproduction for non-commercial purposes, provided the original is properly cited. 

References

- [1] Miyahara S, Uda T, Serizawa M. Prediction of formation of land-tied islands. In: Proceedings of 34th ICCE; 2014. pp. 1-14. https://journals.tdl.org/icce/index.php/icce/article/view/7108/pdf_412
- [2] San-nami T, Uda T, Serizawa M, Miyahara S. Prediction of devastation of natural coral cay by human activity. In: Proceedings of Coastal Dynamics 2013, Paper No. 138; 2013. pp. 1427-1438
- [3] Davis RA, FitzGerald DM. Beaches and Coasts. Malden: Blackwell; 2004. p. 419
- [4] Serizawa M, Uda T, Miyahara S. Interaction between two circular sandy islands on flat shallow seabed owing to waves. In: Proceedings of 34th ICCE; 2014. pp. 1-12. https://journals.tdl.org/icce/index.php/icce/article/view/7106/pdf_410
- [5] Uda T, Serizawa M, Miyahara S. Development of sandbars around islands offshore of Krabi in Thailand and their prediction. In: Proceedings of 36th Conference on Coastal Engineering; 2018 (in press)